Journal of Engineering Science 16(1), 2025, 69-80
DOI: https://doi.org/10.3329/jes.v16i1.82668

JES
an international Journal

EXPERIMENTAL INVESTIGATION ON THE HYDRODYNAMIC PERFORMANCE OF SUBMERGED POROUS TRIANGULAR BREAKWATER

Md. Ashraful Islam[*1], Md. Bashirul Islam[2], Sajjad Ul Haque[1], and Omar Abir[1]

[1]*Department of Water Resources Engineering, Chittagong University of Engineering & Technology, Chattogram-4349, Bangladesh*
[2]*Institute of River, Harbor and Environmental Science, Chittagong University of Engineering & Technology, Chattogram-4349, Bangladesh*

Received: 12 March 2024 Accepted: 10 June 2025

ABSTRACT

This study examines the performance of submerged triangular breakwaters with varying heights and porosities in a two-dimensional wave flume. Experiments were conducted using breakwaters of 10 cm, 12 cm, and 14 cm heights under four wave conditions, with a constant water depth of 15 cm. Water surface elevations were recorded at five locations around the breakwater. Results show that relative breakwater height (h/d) and porosity (n) significantly influence wave transmission. The transmission coefficient (K_t) decreased to a minimum of 0.32 for a solid breakwater at h/d = 0.93. The reflection coefficient (K_r) peaked at 0.43 for a 14 cm solid breakwater. Porosity had minimal effect on reflection but significantly influenced energy dissipation, which reached a maximum (K_d = 0.95) for highly submerged solid breakwaters. Regression analysis confirmed the role of porosity and breakwater width on wave behavior. These findings support the effective design of submerged breakwaters for coastal protection.

Keywords: *Hydrodynamic Performance, Wave Flume, Submerged Triangular Breakwater, Porous Structure, Coastal Protection.*

1. INTRODUCTION

Coastal areas are vital for human activity and economies, supporting marine life, fisheries, and agriculture (Martínez *et al*., 2007). Additionally, they play a key role in tourism and leisure pursuits (Phillips & Jones, 2006). However, these regions face recurring challenges like cyclones, flooding, surges, and erosion (Silva *et al*., 2014), necessitating protective measures to mitigate their impact.

Breakwaters serve as protective barriers against powerful waves in coastal areas and harbours, yet many traditional designs are prone to vulnerabilities. Among various conventional options, the rubble mound breakwater stands out, comprising a malleable trapezoidal structure with quarried rocks at its core and protective artificial armour (Akarsh & Chaudhary, 2023). Its resilience lies in its ability to withstand damage and facilitate easy repairs. However, it is prone to erosion, affecting sediment transport and necessitating regular maintenance. Considering this, submerged breakwaters are available as an alternative. Positioned below water level, they have minimal impact on seabed life, promote water exchange along beaches, and reduce pollution and erosion. Additionally, submerged breakwaters prove effective for navigation.

Various researchers have conducted experimental studies on the hydrodynamic performance of submerged breakwaters. To begin with, Rahman and Womera (2013) analyzed wave interaction with rectangular submerged breakwaters using both experimental and numerical methods. Their results showed that increasing the relative structure height (hs/h) and width (B/L) significantly reduced wave height and energy, with optimal performance observed at hs/h = 0.7 and B/L = 0.3. The SOLA-VOF model they employed achieved over 95% accuracy in surface profile prediction, validating its applicability as a design tool for submerged breakwaters. In a related study, Rahman and Akter (2014) evaluated the hydrodynamic performance of vertical porous breakwaters under varying porosities and wave conditions. Their laboratory experiments revealed that lower porosity and higher submergence ratios effectively minimized wave transmission (Kt = 0.261) and reflection (Kr = 0.089), highlighting the strong influence of porosity and submergence on wave behavior and energy dissipation.

Expanding upon the role of porosity, Chyon *et al*. (2017) examined horizontal slotted submerged breakwaters. Their findings indicated that wave reflection decreased and energy dissipation increased as porosity decreased, with a maximum energy loss of 0.83 recorded at n = 0.4. These results further emphasized the importance of

*Corresponding Author: *md_ashraful@cuet.ac.bd*

ISSN 2075-4914 (print); ISSN 2706-6835 (online)

breakwater geometry and internal structure in wave attenuation. Building on these insights, Afroz and Rahman (2018) employed a two-dimensional numerical model to simulate wave interactions with horizontal slotted breakwaters. Their study demonstrated the ecological benefits of such designs, which enhanced water circulation while maintaining structural efficiency. Model validation against Stokes' third-order wave theory confirmed the reliability of the simulation for sustainable breakwater design. In addition, Zhao *et al*. (2019) explored the interaction of solitary waves with trapezoidal submerged breakwaters. Their study revealed that breakwater slope geometry significantly influenced nonlinear wave behavior, vortex formation, and wave dispersion. A gentler seaward slope enhanced nonlinear effects, while the leeward slope geometry modulated vortex strength and dispersive wave characteristics. Additionally, Mahmoudof and Hajivalie (2021) experimentally investigated the hydraulic performance of smooth impermeable submerged breakwaters under irregular waves. They introduced a new composite dimensionless parameter (β) to predict wave transmission, reflection, and dissipation. Results showed that relative submergence depth had the most significant influence, with β demonstrating strong predictive capability ($R^2 > 0.92$). Rectangular breakwaters were found to be more efficient than trapezoidal ones.

Furthermore, Hasan *et al.* (2022) investigated the use of submerged geotube breakwaters in combination with concrete block revetments for high-energy wave protection. Their results showed that wave energy reduction was closely linked to the relative breakwater height (hb/hw) and width (H/L), with transmission remaining below critical thresholds when breakwater dimensions were optimized. This study proposed an affordable and sustainable two-layer defense system for shoreline stability. In terms of cost-effective design strategies, Magdalena and Jonathan (2022) demonstrated through numerical simulations that increasing the surface roughness of submerged breakwaters was more effective in dissipating resonant energy than increasing structural height. Their findings suggest roughened surfaces provide a practical solution to resonance control in coastal basins. More recently, Wang *et al.* (2023) combined physical experiments and olaFoam modeling to investigate wave evolution over wide permeable breakwaters. The study showed that permeable structures suppressed harmonic generation and turbulent kinetic energy. However, energy dissipation declined beyond a porosity threshold (0.2–0.3), indicating an optimal porosity range for performance.

Peng *et al*. (2024) experimentally assessed dike stability and wave attenuation using combinations of submerged breakwaters, mangroves, and dikes. While submerged breakwaters reduced wave pressure under small waves, they increased water elevation under larger waves, reducing dike stability. Mangroves consistently improved wave attenuation and stability, and their combination with breakwaters was most effective in shallow water but counterproductive in deep water due to amplified wave impacts. Moreover, Al-Towayti *et al.* (2024) evaluated semicircular breakwaters using experiments and simulations, finding that emerged structures (d/h = 0.667) showed the highest reflection (~95%), while alternatively submerged ones (d/h = 1.000) achieved up to 90% energy dissipation. Performance varied with B/L ratio and wave conditions, and the computational model closely matched experimental results. Finally, Wu *et al*. (2025) used a Smoothed Particle Hydrodynamics model with Large Eddy Simulation and particle packing techniques to simulate wave interactions with single and double-submerged semicircular breakwaters. The model showed strong agreement with experimental data for surface elevation, reflection, and transmission coefficients. Results revealed that double breakwaters (DSCB) dissipate more wave energy than single ones (SCB), with energy dissipation concentrated near the first bar during Bragg resonance.

However, studies specifically related to submerged porous triangular breakwaters are scarce, needing further examination. To fill this gap, an analysis of the hydrodynamic performance of a submerged porous triangular breakwater was conducted in a two-dimensional wave tank. This study evaluated the hydrodynamic performance of both porous and solid structures in a triangular submerged breakwater, focusing on the analysis of reflected, transmitted, and absorbed wave energy.

2. METHODOLOGY

2.1 Experimental Setup

The performance of the proposed triangular submerged porous breakwater is being assessed through experiments conducted in a two-dimensional wave flume at the Irrigation Laboratory of Chittagong University of Engineering and Technology (CUET). The flume was 5 meters long, 8 centimeters wide, and 25 centimeters deep. Throughout the study, the bed slope of the flume was zero to maintain a horizontal bed profile. Due to maintaining the control environment, water was staged by using two sluice gates at the upstream and downstream so that no water could leak from the control environment. The breakwater was positioned at a distance of 2.5 meters from the wave generator. At the flume's end, a wave absorber mitigates transmitted waves through the submerged breakwaters. Five wave gauges were set to track water levels at distinct points, and a total of 48 experimental runs were conducted. **Figure 1** illustrates the experimental setup, while **Figure 2** depicts the laboratory flume alongside both solid and porous breakwaters.

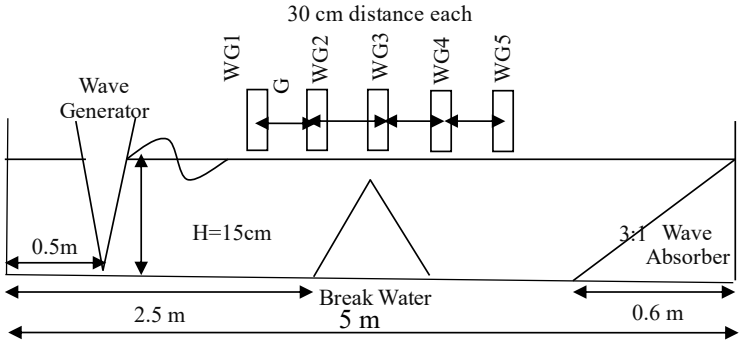

Figure 1: Details of experimental setup.

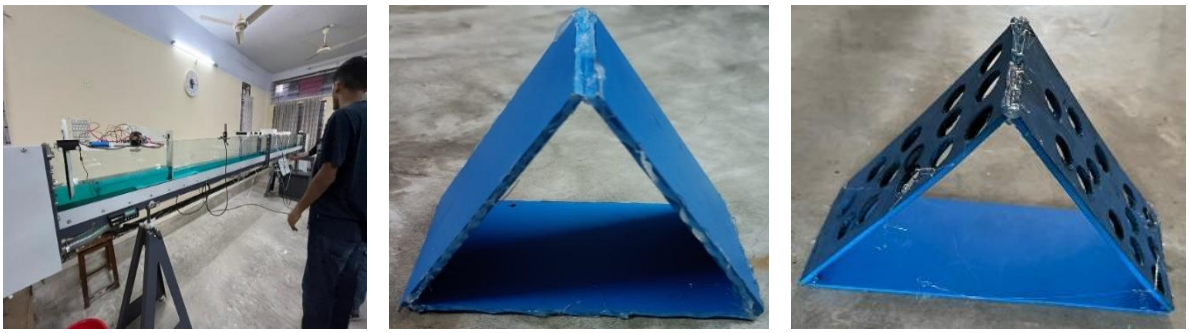

(a) (b) (c)

Figure 2: (a) Laboratory wave flume (left), (b) solid triangular breakwater (middle), and (c) porous triangular breakwater (right).

The wave sponge absorber was positioned at the wave flume's end, spanning 60 centimetres and having a sloped surface with a 3:1 horizontal-to-vertical ratio. Its main purpose is to reduce the number of reflected waves by dispersing the wave energy as they pass through and over the breakwater.

2.2 Triangular Submerged Porous Breakwater

The solid and porous breakwaters, constructed from 4 mm polyvinyl chloride (PVC) sheets, varied in height—10 cm, 12 cm, and 14 cm—resulting in relative submergence (h/d) of 0.67, 0.80, and 0.93, respectively. Each breakwater type, except the solid variants, encompassed three distinct porosity levels. The 10 cm of breakwater had porosities of 28%, 33%, and 40%. Similarly, the 12 cm breakwater exhibited porosities of 26%, 30%, and 38%, while the 14 cm breakwater presented porosities of 20%, 28%, and 35%.

2.3 Experimental Run

Regular waves with varying periods (T) of 0.76 sec, 0.90 sec, 1.2 sec, and 1.5 sec were generated in the wave flume, maintaining a constant still water depth of 15 cm across all runs. The wave generator was adjusted before each run. Water level measurements were taken at five locations for different run conditions, denoted as a, b, c, and d, for periods of T = 1.50, 1.20, 0.90, and 0.76 seconds, respectively. The corresponding wavelengths were 1.74, 1.35, 0.96, and 0.76 meters, respectively, as detailed in **Table 1**, illustrating the test scenarios for the subsequent sections.

2.3.1 Data Collection

This experimental study utilized ultrasonic distance-measuring sensors connected to an Arduino system to monitor wave fluctuations and the temporal changes in water surface elevation. Five sensors were strategically placed at predetermined locations within the experimental setup to record data at each specific point, as illustrated in **Figure 3**. A custom MATLAB-based program was developed to control the Arduino system and enable automatic data acquisition, with its interface shown in **Figure 4**. This setup allowed for water surface elevation data to be collected at a rate of approximately 15 samples per second, providing adequate temporal resolution to capture the wave dynamics effectively.

Table 1: Details of the experimental test scenarios.

Breakwater Properties					Wave Properties		
Still	**Breakwater**	**Submergence,**	**Breakwater**	**Porosity,**	**Time**	**Wave**	**Incident**
0.15	0.10	0.67	0.1155	0 0.28 0.33 0.40	1.50, 1.20, 0.90, and 0.76	1.74, 1.35, 0.96, and 0.76	0.72 ~ 3.31
	0.12	0.80	0.1386	0 0.26 0.30 0.38			
	0.14	0.93	0.1617	0 0.20 0.28 0.35			

To ensure accurate measurements, a thorough calibration of the sensors and the entire measurement system was conducted before the experiments. This process minimized potential errors and ensured reliable data collection. The documented methodology highlights the effective use of advanced instrumentation and custom software to achieve a precise and robust experimental setup for wave height measurement.

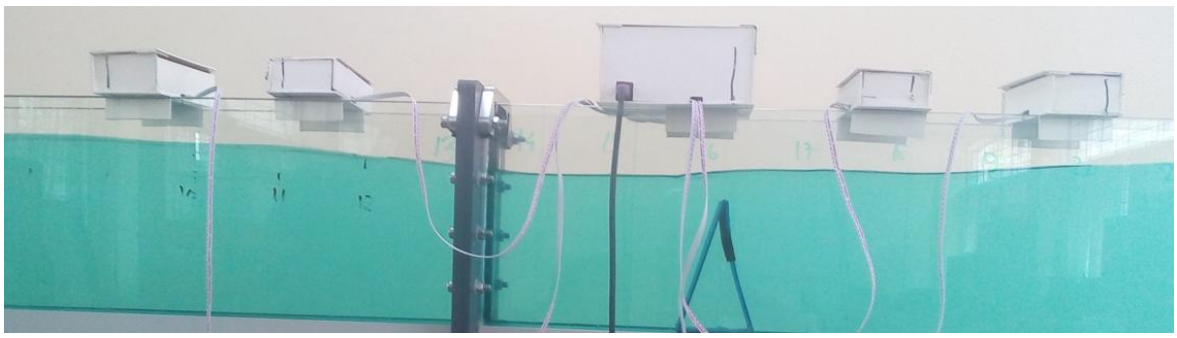

Figure Error! No text of specified style in document.**:** Wave gauge for data collection.

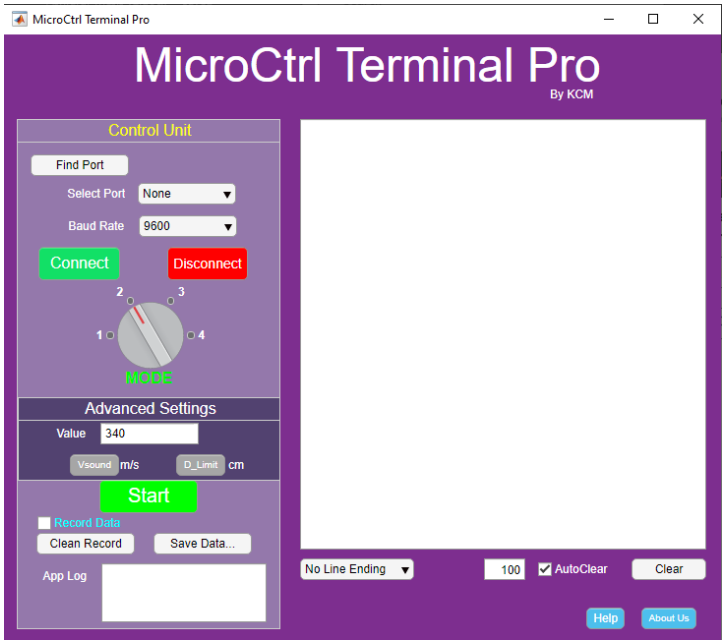

Figure 4: MATLAB-based software program.

2.3.2 Reflection, Transmission, and Dissipation Coefficient Estimation

The reflection (K_r) and transmission coefficients (K_t) of the waves were computed by measuring the maximum (H_{max}) and minimum (H_{min}) wave heights. Those wave heights were captured both upstream (at the wave generator side) and downstream (at the wave absorber side) of the breakwater, following the methods outlined by Goda & Suzuki (1976).

The incident wave height (H_i) and reflected wave height (H_r) were calculated using the following formulas:

$$H_i = (H_{max} + H_{min}) / 2 \quad (1)$$

$$H_r = (H_{max} - H_{min}) / 2 \quad (2)$$

H_{max} represents the maximum wave height, typically measured at antinodes, while H_{min} refers to the minimum wave height, commonly measured at nodes.

The reflection coefficient (K_r) and transmission coefficient (K_t) were calculated using the following formulas:

$$K_r = H_r / H_i \quad (3)$$

$$K_t = H_t / H_i \quad (4)$$

Where H_t is the transmitted wave through the breakwater, and K_L is the energy loss coefficient derived using the relationship ($K_r^2 + K_t^2 + K_L^2 = 1$) established by Thornton & Calhoun (1972).

3. RESULTS AND DISCUSSION

3.1 Comparative Analysis of Water Surface Profiles

The introduction of the solid triangular submerged breakwater has resulted in a reduction in incoming wave energy. In **Figure 5**, the water surface changes at five different points over time are depicted for four distinct wave conditions across the three types of solid triangular breakwaters. It is observed in **Figure 5** that for h = 10 cm with a wave period of T = 1.5 sec, the incident wave height was 1.9 cm, reflecting only 0.4 cm. Approximately 60.5% of the wave's height was transmitted downstream, while 22.2% was reflected. For T = 0.76 sec, the incident wave height increased to 3 cm, with a transmitted wave height of 1.89 cm. The 10 cm triangular solid breakwater reflected only 20% of the incident wave and transmitted 60%. When the submergence depth increased from 66.67% (h = 10 cm) to 80% (h = 12 cm), the transmitted wave decreased to 1.2 cm for longer waves. Conversely, for T = 0.90 seconds, the transmitted wave increased to 2 cm, marking the maximum transmission and reflection coefficients for this breakwater. With a 14 cm breakwater (93% submergence), reflection almost diminished for longer waves and reached about 8% for shorter waves.

a.

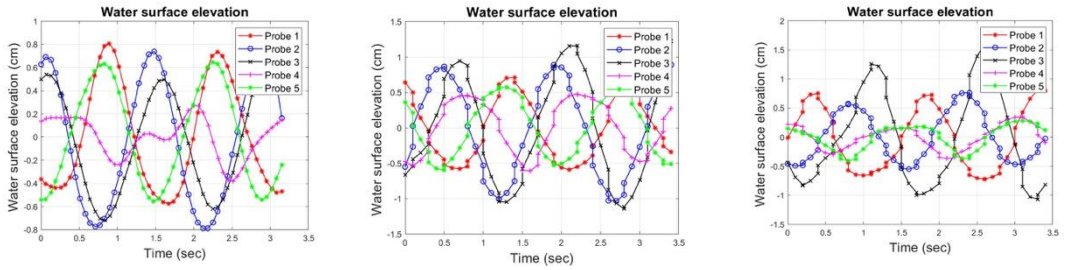

b.

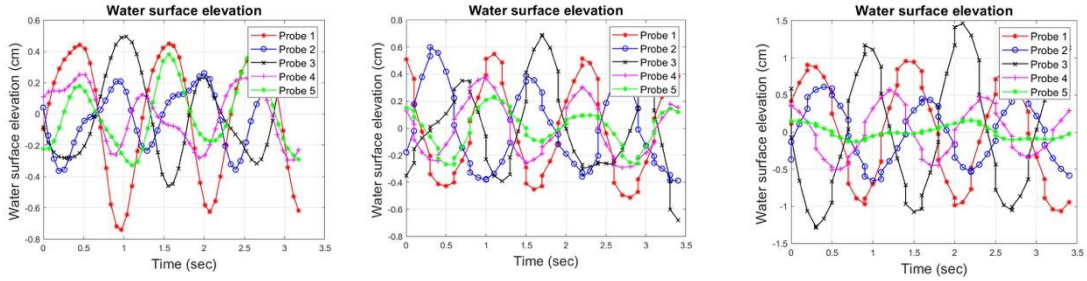

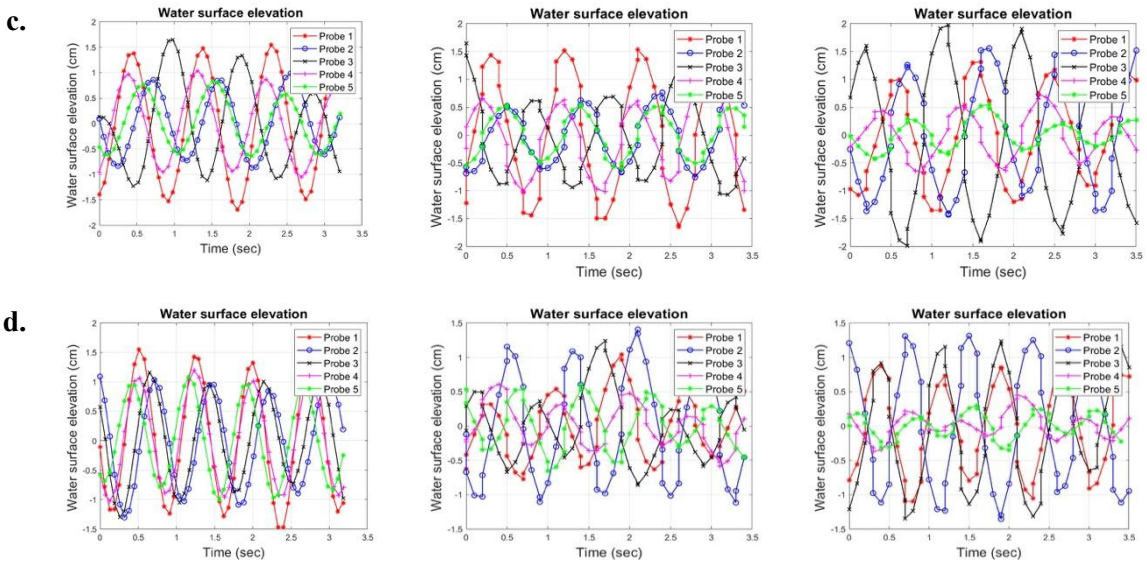

Figure 5: Water surface variation concerning the time at five wave gauge points for (i) 10 cm, (ii) 12 cm, and (iii) 14 cm solid triangular breakwater for four-wave conditions (a, b, c, d).

In **Figure 6**, the incident wave height is 2.0 cm, and it decreases to 1.0 cm after passing through and reflecting off the 28% porous breakwater, resulting in a reflected wave height of 0.63 cm. Simultaneously, the 40% porous breakwater produces 1.5 cm transmitted wave from 1.9 cm incident wave. In contrast, the 33% porous breakwater generates a 0.06 cm reflected wave from a 1.6 cm incident wave for a wave period of T = 1.5 sec.

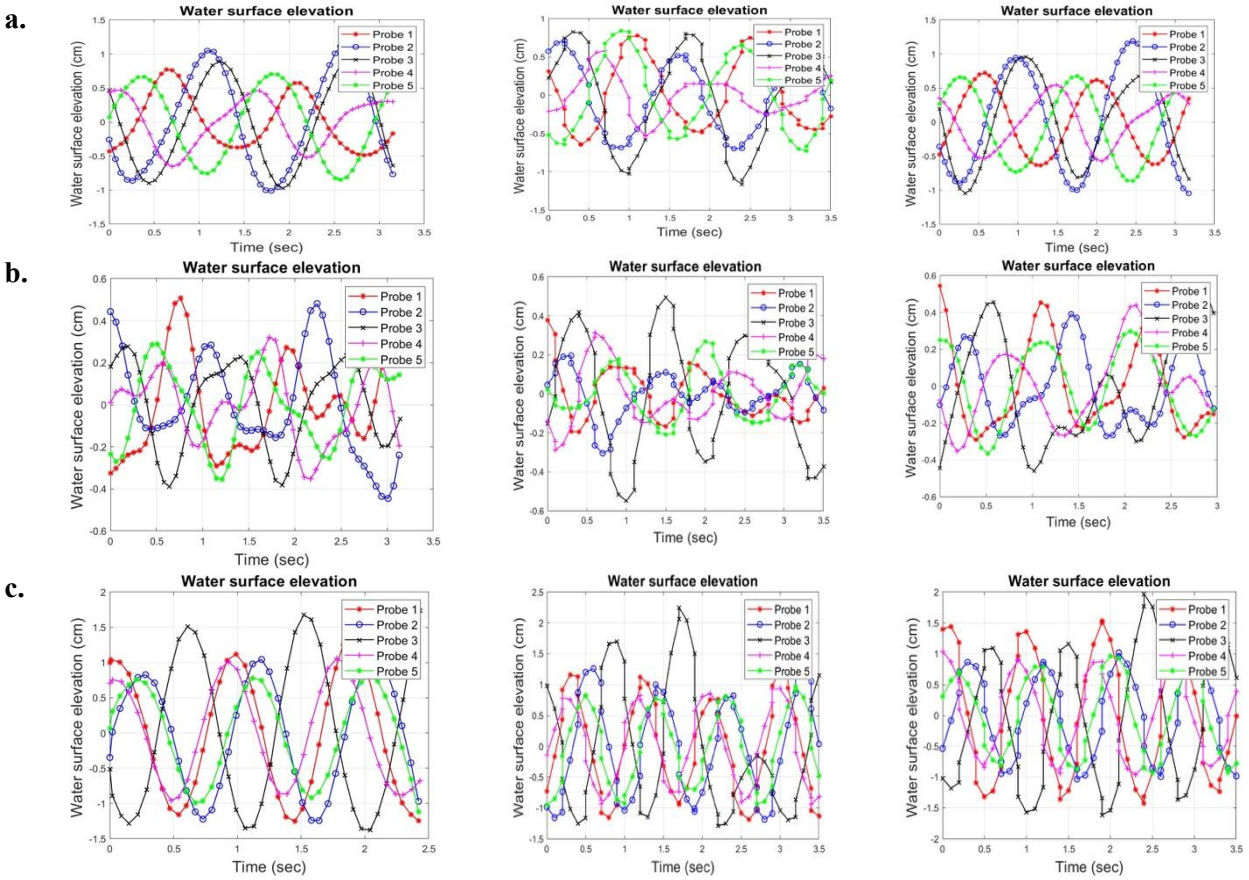

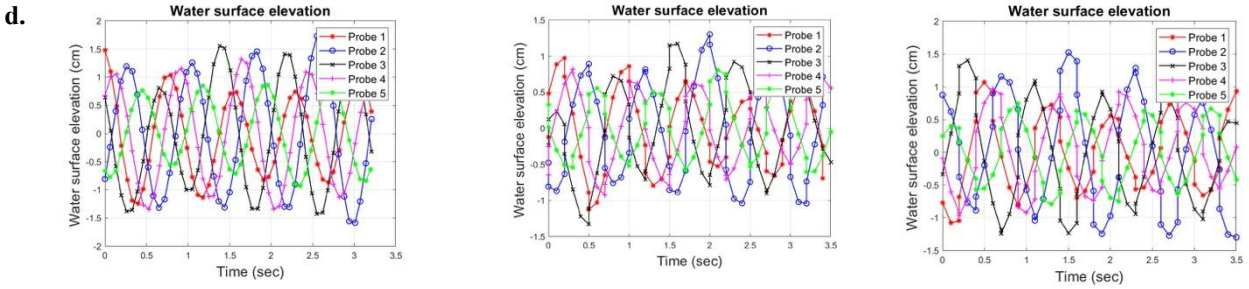

Figure 6: Water surface variation concerning the time at five wave gauge points for 10 cm triangular breakwater with porosities of (i) 0.28, (ii) 0.33, and (iii) 0.40 for four-wave conditions (a, b, c, d).

In **Figure 7**, the transmitted wave height for the porous breakwater (h = 12 cm) is notably lower. It measures only 1.4 cm for porosity of 0.26 and 1.3 cm for porosity of 0.30 for a wave period of T = 1.5 sec. Nearly 30% of the wave is reflected from the 38% porous triangular submerged breakwater. Meanwhile, as shown in **Figure 8**, the transmitted wave height is lower compared to other breakwater types. The reflected wave increases due to the increased breakwater submergence. Also, reflection rises with decreasing porosity for the 1.5 sec wave period. Specifically, the transmitted wave height measures 1.5 cm for 35% porous breakwater, higher than the 1.3 cm observed with 20% porous breakwater.

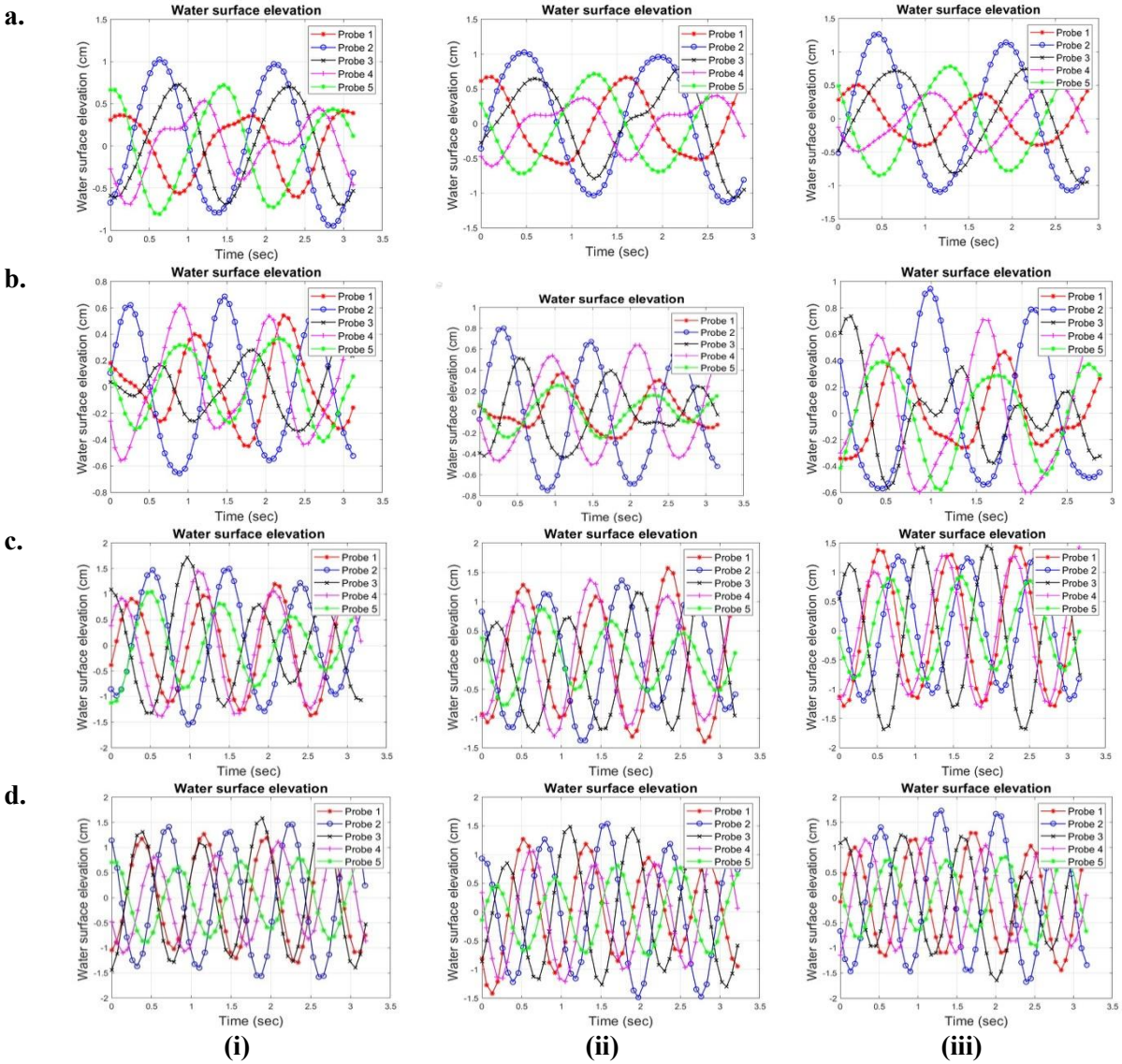

Figure 7: Water surface variation concerning the time at five wave gauge points for 12 cm triangular breakwater with porosities of (i) 0.26, (ii) 0.30, and (iii) 0.38 for four-wave conditions (a, b, c, d).

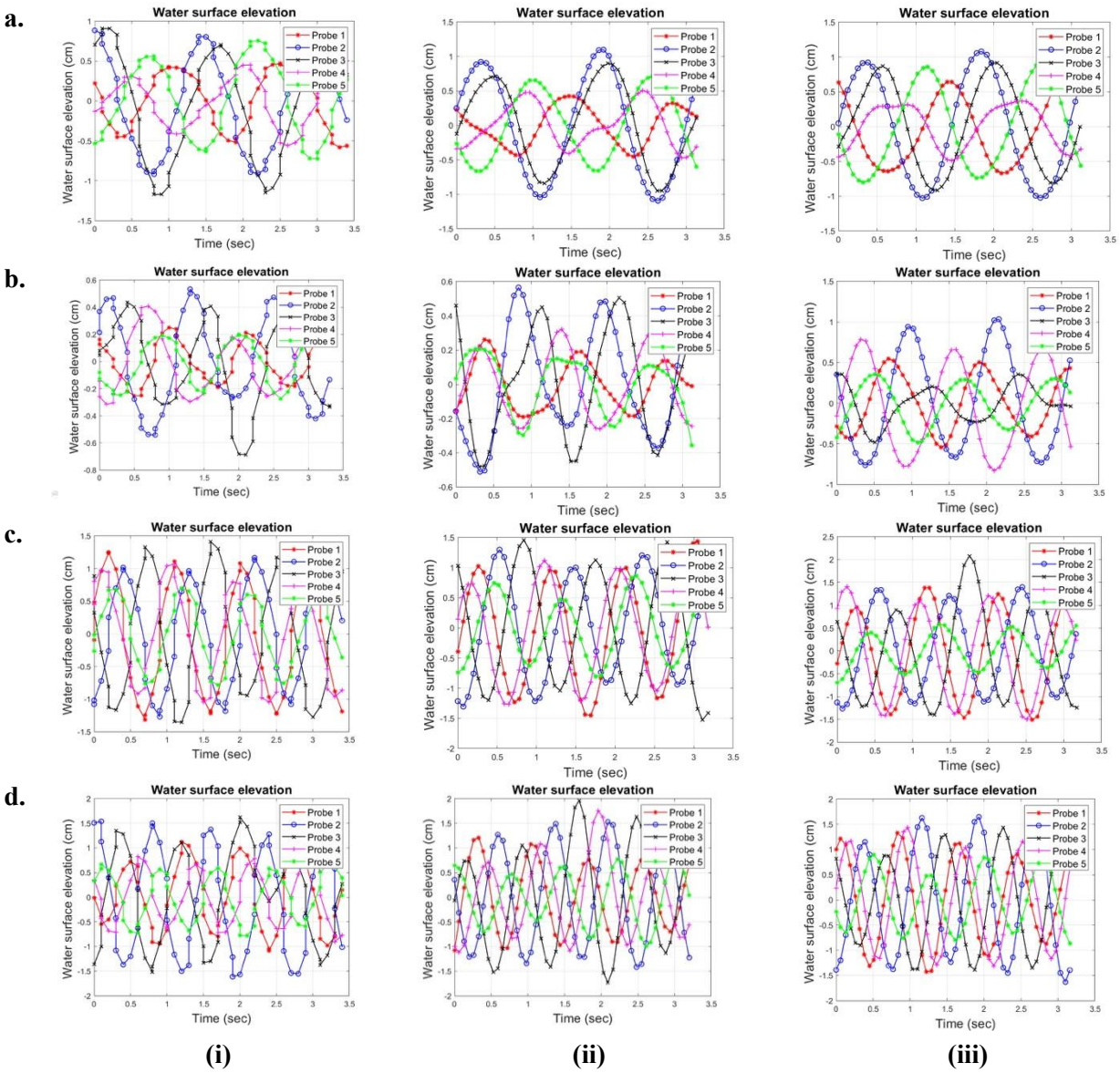

Figure 8: Water surface variation concerning the time at five wave gauge points for 14 cm triangular breakwater with porosities of (i) 0.20, (ii) 0.28, and (iii) 0.35 for four-wave conditions (a, b, c, d).

The water surface variation observed for probe 3 displays a non-sinusoidal pattern over time (see **Figures 5-8**), indicating non-linearity generated primarily at the breakwater due to energy dissipation. This pattern suggests that an increase in submergence leads to decreased wave transmission but increased wave reflection. Conversely, an increase in porosity decreases reflection but increases wave transmission.

3.2 Impact of Relative Submergence (h/d) and Relative Breakwater Width (B/L) on Wave Transmission Coefficient, K_t

Figure 9(a) depicts the correlation between the transmission coefficient (Kt) and the relative breakwater width (B/L) for three triangular solid breakwaters with submergences (h/d) of 0.92, 0.80, and 0.67. Generally, as the relative breakwater width increases, the transmission coefficient (Kt) decreases across most cases, indicating the width's impact on reducing transmitted waves. This behavior might be attributed to increased friction between the wider breakwater and transmitted waves, resulting in greater energy loss. Moreover, when waves encounter this wider structure, abrupt changes in water particle velocity and acceleration occur, generating turbulence that dissipates wave energy. In **Figure 9**(a), it is shown that the transmission coefficient (Kt) decreases with higher submergences. The lowest transmission coefficient (Kt) is observed at h/d = 0.93, indicating its effectiveness in interacting with most waves. Specifically, 14 cm of solid triangular breakwater at a B/L of 0.21 achieves a minimum transmission coefficient (Kt) of 0.32, creating a calmer leeward side. For 93% submergence, Kt ranges

from 0.32 to 0.44; for 80% submergence, it's between 0.42 and 0.72; and for 67% submergence, it varies from 0.6 to 0.78.

Figures 10(a), (b), and (c) depict the impact of porosity on wave transmission through the porous breakwater. Across all cases, it is shown that wave transmission coefficients decrease as the relative breakwater width (B/L) increases. Additionally, increases in porosity lead to higher wave transmission rates. Specifically, transmission coefficients vary between 0.60 and 0.85 for 67% submergence but only between 0.33 and 0.85 for 93% submergence. This indicates that while porosity influences wave transmission, the depth of submergence has a more substantial impact on the transmission of incident waves across all scenarios.

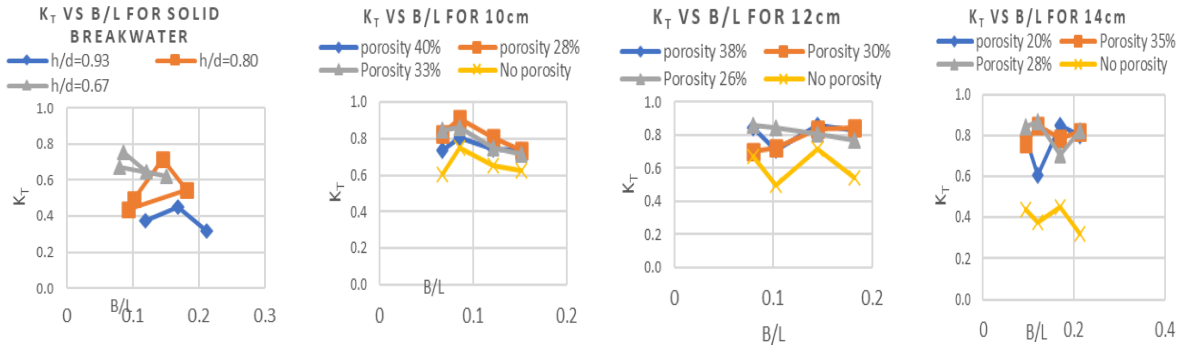

Figure 9: Effect of relative breakwater width (B/L) on transmission coefficient (Kt) for (a) solid breakwaters, (b) 10 cm, (c) 12 cm, and (d) 14 cm breakwater.

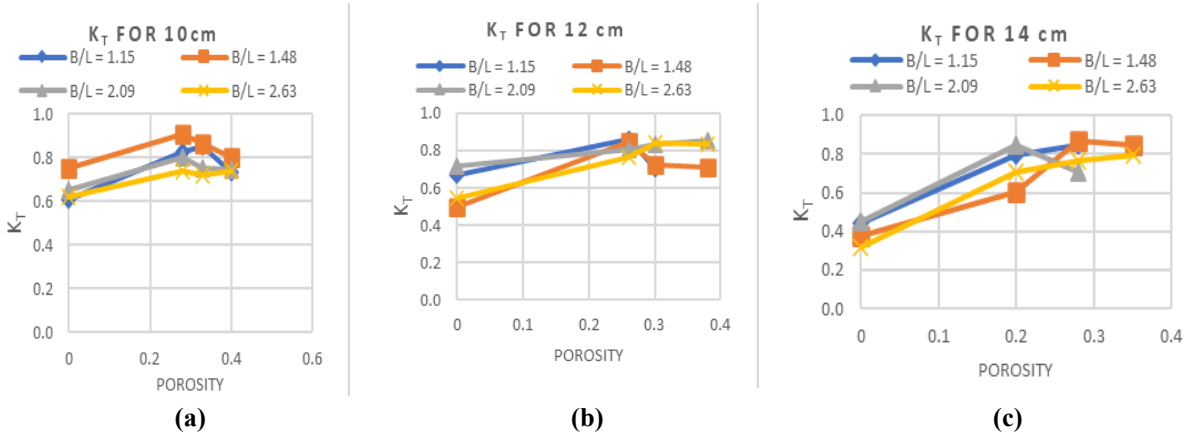

Figure 10: Effect of porosity on transmission coefficient (Kt) for (a) 10 cm, (b) 12 cm, and (c) 14 cm breakwater.

3.3 Impact of Relative Submergence (h/d) and Relative Breakwater Width (B/L) on Wave Reflection Coefficient, K_r

Figure 11 demonstrates the relationship between reflection coefficients (Kr) and relative breakwater width (B/L). Minimum reflection occurs for low-submerged, high-porosity breakwaters, particularly for a 10 cm breakwater with 40% porosity. In **Figures 11**(a)-(d), Kr demonstrates a negative correlation with B/L: an increase in B/L leads to a decrease in the reflection coefficient. The maximum reflection coefficient is observed for a 14 cm solid triangular breakwater with 93% submergence. Reflection coefficients range from near zero to 40% for different porosities. In **Figure 12**, porosity displays a negative relationship with wave reflections; as porosity increases, the reflection coefficient decreases. Additionally, while Kr increases with decreasing relative breakwater width (B/L), its impact on wave reflections is relatively minor.

3.4 Impact of Relative Submergence (h/d) and Relative Breakwater Width (B/L) on Wave Energy Dissipation Coefficient, K_d

In **Figure 13**(a), it is shown that the energy dissipation coefficient (Kd) varies from 0.6 to 0.95 for solid-type breakwaters. With an increase in the relative breakwater width (B/L), energy dissipation (Kd) also increases due to the larger breakwater base interacting more with waves and dissipating more energy. Additionally, Kd ranges

from 0.6 to 0.75 for h/d of 0.67, 0.63 to 0.88 for h/d of 0.80, and 0.90 to 0.95 for h/d of 0.93. This suggests that a higher depth of submergence dissipates more wave energy than a lower breakwater. Notably, the majority of the wave energy concentrates near the surface, dissipating as the breakwater height increases. In **Figure 13**(b), it is shown that for a 10 cm breakwater height, the minimum energy dissipation coefficient (Kd) is observed at a B/L of 0.093 for both porous and solid breakwaters. This figure also illustrates that the energy coefficient varies between 0.4 and 0.78 for 10 cm of triangular breakwater. However, for 14 cm triangular breakwater, this coefficient ranges from 0.35 to 0.95, indicating that increased submergence widens the spectrum of energy dissipation. Additionally, **Figure 13**(b) shows that the energy dissipation coefficient (Kd) ranges from 0.4 to 0.85, leading to the conclusion that an increase in submergence indeed expands the range of energy dissipation possibilities.

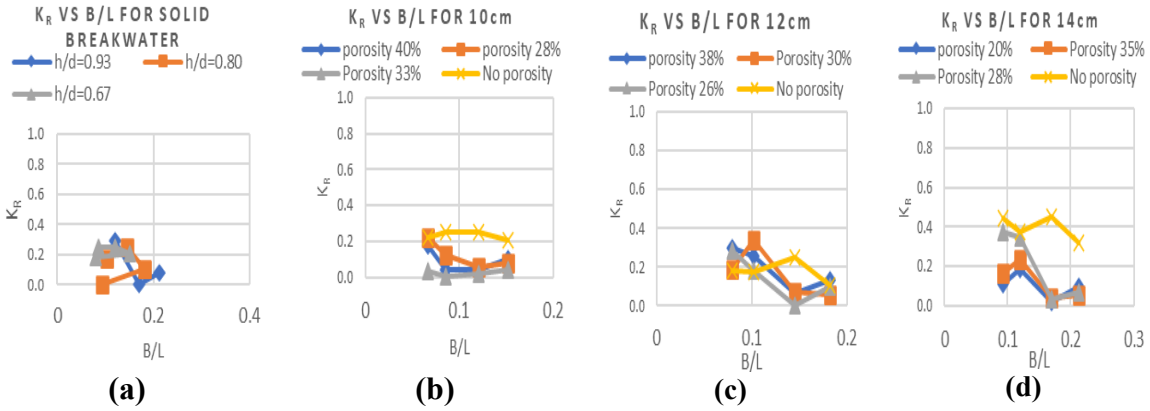

Figure 11: Effect of relative breakwater width (B/L) on reflection coefficient (Kt) for (a) solid breakwaters, (b) 10 cm, (c) 12 cm, and (d) 14 cm breakwater.

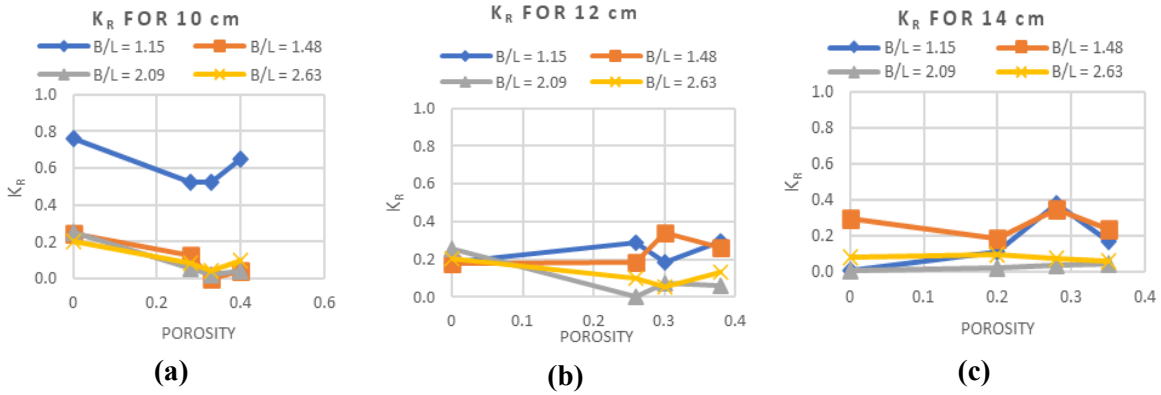

Figure 12: Effect of porosity on reflection coefficient (Kr) for (a) 10 cm, (b) 12 cm, and (c) 14 cm breakwater.

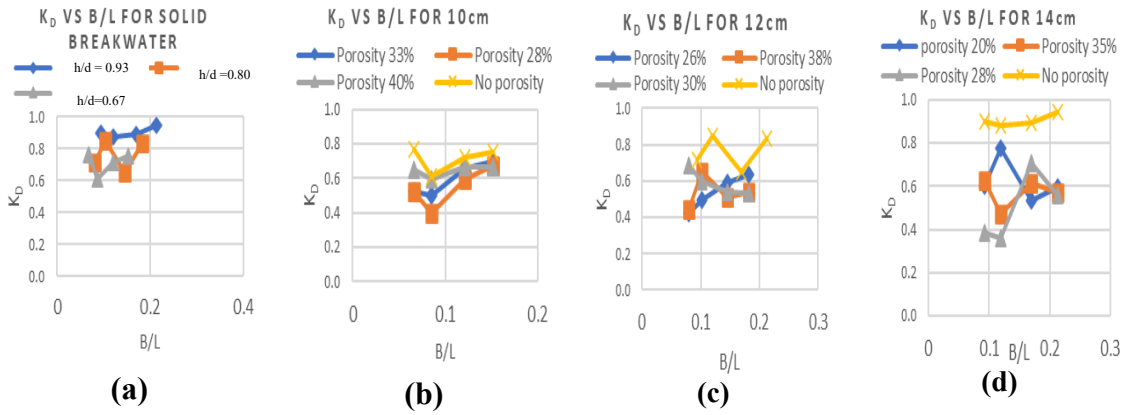

Figure 13: Effect of relative breakwater width (B/L) on energy dissipation coefficient (Kt) for (a) solid breakwaters, (b) 10 cm, (c) 12 cm, and (d) 14 cm breakwater.

In **Figure 14**, it is shown that the energy dissipation coefficient (Kd) varies with increasing porosity across all three types of submerged triangular breakwaters. In **Figure 14**(a), there is a slight decrease in Kd with increasing porosity for a submergence of 0.67. However, Kd moderately decreases with rising porosity for a submergence of 0.80. Particularly, the energy dissipation coefficient decreases from 0.95 to 0.35 with an increase in porosity from 0 to 0.28. This suggests that porosity has a more substantial impact on energy dissipation for larger submerged triangular breakwaters.

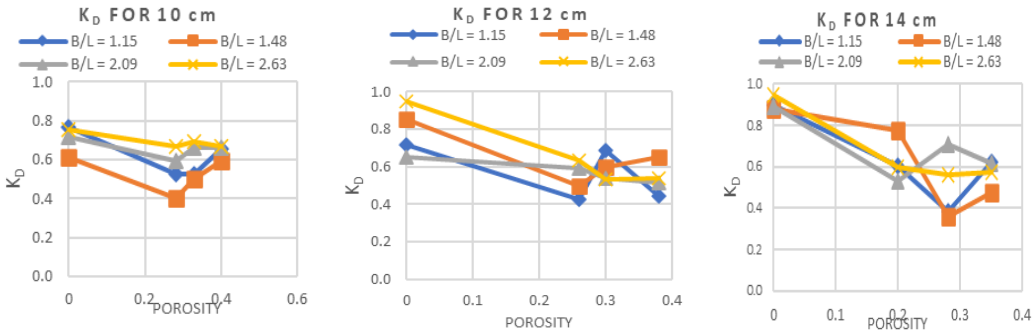

Figure 14: Effect of porosity on energy dissipation coefficient (Kt) for (a) 10 cm, (b) 12 cm, and (c) 14 cm breakwater.

3.5 Regression Analysis

Developing equations from observed data involves utilizing multiple regression analysis using the least squares method to establish connections between dimensionless coefficients obtained through measurements. These equations specifically relate the transmission coefficient, reflection coefficient, and energy dissipation coefficient concerning factors like the relative breakwater width (B/L), submergence ratio (h/d), and porosity (n) for regular waves. This statistical approach allows for the formulation of predictive equations based on the gathered empirical data, facilitating a quantitative understanding of how these coefficients vary concerning the specified parameters.

$$Kt = 0.844 - 0.308\,(B/L) - 0.276\,(h/d) + 0.662n\ (R^2 = 0.582) \quad (5)$$

$$Kr = 0.276 - 0.997(B/L) - 0.056(h/d) - 0.138n\ (R^2 = 0.237) \quad (6)$$

$$Kd = 0.531 + 0.640(B/L) + 0.184(h/d) - 0.628n\ (R^2 = 0.486) \quad (7)$$

The analysis reveals that Equation (5) shows an acceptable correlation (R^2 = 0.582) between the transmission coefficient and B/L, h/d, and n. Increasing B/L and h/d reduces transmission, while porosity exhibits a positive correlation with wave transmission. However, Equation (6) with an R^2 of 0.237 doesn't demonstrate an acceptable linear correlation with wave reflection, indicating a need for further research in this field. On the other hand, Equation (7) with an R^2 value of 0.486, very close to the acceptable range, signifies a correlation between energy dissipation and relative breakwater width, submergence ratio, and porosity. The coefficient of porosity (-0.628) in Equation (7) indicates a strong negative influence on energy dissipation, while the relative breakwater width shows a positive influence with a coefficient of 0.640.

4. CONCLUSIONS

The experimental investigation explored the hydrodynamic behavior of submerged porous triangular breakwaters under regular wave action. The study conducted 48 laboratory runs in a two-dimensional wave flume involving different submergence conditions. Wave patterns indicated sinusoidal behavior before and after the breakwater but showed non-sinusoidal patterns near and on the breakwater due to vortex formation and energy dissipation. This study found a decrease in the transmission coefficient (Kt) with increasing relative breakwater width, transmitting a minimum of 32% of the incident wave for a solid triangular breakwater with an h/d of 0.93. Porosity had a more pronounced impact on highly submerged breakwaters compared to those with lower submergence. On the other hand, the reflection coefficient (Kr) increased with higher breakwater height and decreased relative width, peaking at 0.43 for a solid 14 cm triangular breakwater, while porosity minimally affects wave reflection. Energy dissipation increases with the B/L ratio but decreases with higher porosity, reaching a maximum (Kd = 0.95) for highly submerged solid triangular breakwaters, where porosity notably affects energy dissipation. The triangular breakwater, featuring variable porosity from 0% to 20% and submerged at 93% (for 14 cm of breakwater), is suggested as an effective choice for shielding coastal areas against similar wave conditions.

Regression analysis highlighted the influence of relative breakwater width, porosity, and submergence ratio on the wave behavior. These findings could aid coastal engineers in efficiently designing porous submerged triangular breakwaters for various applications.

ACKNOWLEDGEMENT

The authors gratefully acknowledge the invaluable support and assistance provided by all laboratory staff of the Irrigation Laboratory of the Department of Water Resources Engineering, Chittagong University of Engineering and Technology (CUET).

REFERENCES

Afroz, R., & Rahman, M. A. (2018). Numerical Simulation of Wave Interaction with Horizontal Slotted Submerged Breakwater. *Global Science and Technology Journal, 6*(3), 1–11.

Akarsh, P. K., & Chaudhary, B. (2023). *Review of Literature on Design of Rubble Mound Breakwaters* (pp. 775–796).

Al-Towayti, F. A. H., Teh, H. M., Ma, Z., Jae, I. A., Syamsir, A., & Al-Qadami, E. H. H. (2024). Hydrodynamic Performance Assessment of Emerged, Alternatively Submerged and Submerged Semicircular Breakwater: An Experimental and Computational Study. *Journal of Marine Science and Engineering 2024, 12*(7), 1105.

Chyon, M. S. A., Rahman, A., & Rahman, M. A. (2017). Comparative Study on Hydrodynamic Performance of Porous and Non-Porous Submerged Breakwater. *Procedia Engineering*, *194*, 203–210.

Goda, Y., & Suzuki, Y. (1976). Estimation of Incident and Reflected Waves in Random Wave Experiments. In *Coastal Engineering* (pp. 828–845).

Hasan, M. K., Rahman, M. A., & Womera, S. Al. (2022). Experimental Study on the Stability of Concrete Block Revetment for High Waves Propagating over Submerged Geotube Breakwater. *International Journal of Coastal, Offshore and Environmental Engineering (Ijcoe)*, *7*(1), 15–22.

Magdalena, I., & Jonathan, G. (2022). Water waves resonance and its interaction with submerged breakwater. *Results in Engineering*, *13*, 100343.

Mahmoudof, S. M., & Hajivalie, F. (2021). Experimental study of hydraulic response of smooth submerged breakwaters to irregular waves. *Oceanologia*, *63*(4), 448–462.

Martínez, M. L., Intralawan, A., Vázquez, G., Pérez-Maqueo, O., Sutton, P., & Landgrave, R. (2007). The coasts of our world: Ecological, economic and social importance. *Ecological Economics*, *63*(2–3), 254–272.

Peng, M., Zhang, J., Zhu, Y., Gao, L., Li, S., & Pan, X. (2024). Experimental study on wave attenuation and stability of ecological dike system composed of submerged breakwater, mangrove, and dike under storm surge. *Applied Ocean Research*, *151*, 104144.

Phillips, M. R., & Jones, A. L. (2006). Erosion and tourism infrastructure in the coastal zone: Problems, consequences and management. *Tourism Management*, *27*(3), 517–524.

Rahman, M. A., & Akter, A. (2014). The Effect of Porosity of Submerged and Emerged Breakwater on Wave Transmission. *International Journal of Environmental Science and Development*, *5*(5), 473–478.

Rahman, M. A., & Womera, S. (2013). Experimental and Numerical Investigation on Wave Interaction with Submerged Breakwater. *Journal of Water Resources and Ocean Science*, *2*(6), 155.

Silva, R., Martínez, M. L., Hesp, P. A., Catalan, P., Osorio, A. F., Martell, R., Fossati, M., Da Silva, G. M., Mariño-Tapia, I., Pereira, P., Cienguegos, R., Klein, A., & Govaere, G. (2014). Present and future challenges of coastal erosion in Latin America. *Journal of Coastal Research*, *71 (10071)*, 1–16.

Thornton, E. B., & Calhoun, R. J. (1972). Spectral Resolution of Breakwater Reflected Waves. *Journal of the Waterways, Harbors and Coastal Engineering Division*, *98*(4), 443–460.

Wang, P., Fang, K., Wang, G., Liu, Z., & Sun, J. (2023). Experimental and Numerical Study of the Nonlinear Evolution of Regular Waves over a Permeable Submerged Breakwater. *Journal of Marine Science and Engineering*, *11*(8), 1610.

Wu, X. Y., Liu, X., Chen, Y. K., & Liu, Y. (2025). Wave energy evolution during Bragg resonance reflection of waves interaction with submerged semicircular breakwaters through the smoothed particle hydrodynamics. *Physics of Fluids*, *37*(2).

Zhao, X. L., Ning, D. Z., Zou, Q. P., Qiao, D. S., & Cai, S. Q. (2019). Hybrid Floating Breakwater-WEC System: A Review. *Ocean Engineering*, *186*, 106126.

© 2025 JES. *Journal of Engineering Science published by the Faculty of Civil Engineering, Khulna University of Engineering & Technology*. This is an open access article under the terms of the Creative Commons Attribution-Noncommercial-No Derivatives License, which permits use and distribution in any medium, provided the original work is properly cited, the use is non-commercial and no Modifications or adaptations are made.